

The Fate of Inflaton Fluctuations in Multi-field Scenarios During Inflation



Frédéric Mouton

This thesis is submitted in partial fulfillment
of the requirements for the degree of
Master of Science
October 2015

Contents

1	Introduction	7
2	Cosmological Inflation	9
2.1	The Hot Big Bang Model	9
2.2	The Shortcomings of the Hot Big Bang Model	10
2.2.1	The Flatness Problem	10
2.2.2	The Horizon Problem	12
2.2.3	The Monopole Problem	12
2.3	Cosmological Inflation	15
2.4	Scalar Field Inflation	16
3	Field Fluctuations in a Time Dependent Background	19
3.1	Inhomogeneous Universe	19
3.2	The Klein-Gordon Equation	20
3.2.1	The Klein-Gordon Equation in Flat Space-Time	20
3.2.2	The Klein-Gordon Equation in Curved Space-Time	21
3.3	Quantum Fluctuations of a Massless Scalar Field	22
4	Inflaton fluctuations in multi-field scenarios	26
4.1	Motivations	26
4.2	Field Equations and the Stochastic Approach	28
4.3	The Window Function and the Noise Correlators	31
4.4	Numerical Analysis	33
4.4.1	Setup	33
4.4.2	Numerical Simulations	35
4.4.3	Numerical Analysis	36
4.4.4	Preliminary results	38
4.4.5	Numerical Results	41

List of Figures

2.1	The solid line illustrates the potential when $\psi = 0$, while the dashed line shows the potential with $\psi^2 > m^2/\lambda_2$. From [10].	14
2.2	Schematic of the inflationary solution to the horizon problem. From [1].	16
4.1	The potential shown in equation 4.16 (All variables are dimensionless, as detailed in (4.12).)	38
4.2	Time evolution of the flat and non-flat directions according to [14] . . .	39
4.3	Time evolution of the flat and non-flat directions according to [15] . . .	40
4.4	Evolution of the variances of the infrared modes for $\lambda = g = 1$ and $\frac{H^2}{M_{pl}^2} = 10^{-10}$	43
4.5	Evolution of the masses of the flat Φ and non-flat χ directions for $\lambda = 1$ and $\frac{H^2}{M_{pl}^2} = 10^{-10}$	45
4.6	Integrated noise correlation function $\langle S_\phi \rangle$ averaged over the number of runs.	46
4.7	Integrated noise correlation function $\langle S_\pi \rangle$ averaged over the number of runs.	46
4.8	Evolution of the variance of the flat direction Φ for $\lambda = 1$ and varying $\frac{H^2}{M_{pl}^2}$	48
4.9	Evolution of the variance of the flat Φ and non-flat χ directions for $\lambda = 1$ and $\frac{H^2}{M_{pl}^2} = 0$	49

Abstract

The Fate of Inflaton Fluctuations in Multi-field Scenarios During Inflation

Frederic Mouton

October 2015

In this thesis, we give an introductory account of inflationary cosmology. We explain how a period of accelerated expansion in the Universe's early stages can explain some paradoxes encountered in cosmology. Furthermore, we study the quantum fluctuations of a generic scalar field during inflation while putting the emphasis on the different behaviour of the fluctuations in or out of the horizon. Finally, we consider an inflationary potential composed of two coupled scalar fields: one flat direction and a non-flat one. We solve the Langevin equations numerically for these two fields and contrast our results and approach with two previous studies. We find that the fluctuations of the flat direction does not saturate in the range of e-folds considered.

Declaration

This thesis has been composed by myself and no portion has been submitted in support of an application for another degree or qualification of this or any other university or other institute of learning. This work was carried out within the Cosmology and Astroparticle Physics Group at Lancaster University.

I, hereby, grant the University of Lancaster the right to retain a copy of this thesis, either physically or electronically.

Acknowledgments

I would like take this opportunity to express my gratitude to everyone who supported me throughout this degree. I would like to thank the Department of Physics and its staff for the opportunity to undertake this research and for their help in all the administrative matters. In particular, I would like to express my special appreciation and thanks to my supervisor Dr Dimopoulos for his guidance and patience. I would also like to thank my fellow students in the theory group for the cheerfulness they brought to this year of hard work.

Outside of Lancaster, I would like to thank Profs Neil Spooner and Jocelyn Monroe for their trust and the opportunity to continue my studies.

A special acknowledgment goes to my parents, whose constant support and firm determination have always been two shoulders to stand upon during my moments of doubt. I would also like to thank them for valuing my education above all else. Last but not least, I would like to thank Mathilde for offering me a patient hear and a comforting smile everyday, and also for coping with the boredom of reading every single report I have written since I started university.

Chapter 1

Introduction

The precise measurement of the Cosmic Microwave Background has transformed research in cosmology and it is claimed that it started a “Golden Age of Cosmology”. While the origin of the Universe is a question as old as mankind, the recent cosmological surveys have brought a large quantity of data which is now studied to obtain this ultimate answer. The Cosmic Microwave Background is, for now, the only clue to study inflation: a period of exponential expansion of the Universe supposed to have begun when it was around 10^{-42} seconds old [1].

It is now accepted that a Hot Big Bang produced a plasma of particles cooling down due to the expansion of the Universe. The decoupling of these particles, in particular photons and electrons, has made the Universe transparent and has allowed these photons to travel to us freely. The Cosmic Microwave Background is therefore an imprint of the early Universe in which it is believed that many clues are hidden, such as gravitational waves and traces of an inflationary period [1].

During inflation, the small quantum perturbations are stretched by the expansion and amplified into the classical density perturbations which are

believed to be the origin of the large scale structure in the Universe [1]. Understanding them is an important aspect of early Universe cosmology. Flat directions are directions in field space where the potential is constant. In this situation, the field can vary at no cost in energy and may acquire a large vacuum expectation value. Since the inflaton field is a flat direction of the inflationary potential it is interesting to see the evolution of flat directions in multi-field scenarios. This thesis considers the inflationary trajectory and studies its evolution to find whether it may indeed have large fluctuations.

Chapter 2 recalls the inflationary paradigm. It exposes some of the problems in cosmology and briefly shows how inflation can solve them.

Chapter 3 describes the quantum perturbations in the inflationary epoch while focusing on the difference between infrared and ultraviolet modes.

Chapter 4, finally, describes eternal inflation and reviews the stochastic equations used in our computer simulations to study the time evolution of a flat direction in a multi-field case during inflation. The results obtained are compared with two previous similar studies.

Chapter 2

Cosmological Inflation

2.1 The Hot Big Bang Model

The Hot Big Bang Model is overall a successful model. It is capable of explaining most of the key features observed in the Universe. This model is based on the observations by Hubble in 1924 [2] that the redshift of galaxies is proportional to their distances. This result, known as Hubble's Law, combined with the Cosmological Principle (the assumption that the Universe is homogeneous and isotropic), implies that the Universe must have previously been smaller and denser. This deduction is reinforced by the observation of the Cosmic Microwave Background (CMB) which proves that the Universe was previously hot. The facts that the CMB is blackbody radiation and that the temperature anisotropies are small $\Delta T/T \sim 10^{-5}$ [8] also support the Cosmological Principle.

Another strength of the Hot Big Bang model is the account it gives of the formation of the light elements and its ability to predict their correct abundances. Nucleosynthesis was believed to happen when the Universe was around one second old at a temperature of $T \approx 10^{10}\text{K}$ [6]. At this time, the temperature has cooled enough to allow the nuclear fusion of protons and

neutrons into Hydrogen and Helium nuclei. As the Universe continued to expand, the temperature cooled down below the required level and the fusion process is frozen out. At this point, the density of the light elements is fixed.

The following era is called the radiation era. Since the binding energy between a nucleus and its electrons is less than the strong force between the nuclei themselves, electrons remain free in the original opaque plasma. At around $T \approx 1\text{eV}$, recombination happens [6]. Electrons become bound to the nuclei to form atoms. At this point, photons can travel freely from the surface of last scattering and the Universe becomes transparent. These photons are cooled to 2.7K and redshifted to the microwave scale due to the expansion of the Universe to become the Cosmic Microwave Background that we observe today [6]. This marks the beginning of the matter dominated era.

2.2 The Shortcomings of the Hot Big Bang Model

Despite its success, the Hot Big Bang model also has its limitations. Dark matter, dark energy and inflation have become widely accepted additions to the model. Inflation, in particular, was proposed as a solution to the horizon, flatness and monopole problems, which are described below. This small review is mainly based on [3, 6].

2.2.1 The Flatness Problem

The flatness problem refers to the fact that the density of the Universe is close to its critical density. The critical density ρ_{crit} is the density for which the Universe has just enough energy to prevent contraction into a

Big Crunch due to its own gravitational attraction. This is known as the Einstein - deSitter model. Using the Friedmann Equation:

$$H^2 = \left(\frac{\dot{a}}{a}\right)^2 = \frac{8\pi G\rho}{3} - \frac{kc^2}{a^2}, \quad (2.1)$$

it is possible to define the critical density for which the Universe is flat (i.e. $k = 0$):

$$\rho_{crit} = \frac{3H^2}{8\pi G}, \quad (2.2)$$

where $H = \dot{a}/a$ is the Hubble parameter and G is the gravitational constant.

The density parameter $\Omega_{tot} = \frac{\rho}{\rho_{crit}}$ is therefore 1 when the Universe is flat. The subscript “tot” denotes the fact that the density parameter can be separated into its different constituents ($\Omega_{matter}, \Omega_{radiation}...$ etc). The current density parameter $\Omega_{tot} = 0.9995 \pm 0.0034$ can be measured experimentally from the observation of the CMB [4, 5]. Using Friedmann’s equation (2.1), it can be related to the curvature index k :

$$|\Omega_{tot} - 1| = \frac{|k|c^2}{a^2H^2}. \quad (2.3)$$

The flatness problem lies in the fact that in order for the density parameter to be close to 1 today, it must have been even closer to 1 before. This is because for radiation $a \sim t^{1/2}$ and $a \sim t^{2/3}$ for matter, so $|\Omega_{tot} - 1|$ increases as the Universe gets older. It is estimated that at the electro-weak symmetry breaking scale ($t \simeq 10^{-12}$ s), we need $|\Omega_{tot} - 1| \leq 10^{-30}$ [6]. This level of fine tuning is considered unphysical.

2.2.2 The Horizon Problem

The key idea behind the horizon problem is that both the speed of light and the age of the Universe are finite, so a photon can only have traveled a finite distance during the lifespan of the Universe. This distance is known as the particle horizon. Consequently, two particles separated by a distance larger than their particle horizons cannot have been in contact with each other and there shouldn't be any correlation between their physical properties.

The distance to the particle horizon R_H can be derived from the FLRW metric and is given by [7]:

$$R_H(t) = a(t) \int_0^t \frac{dt'}{a(t')} = a \int_0^a \frac{da}{a} \left(\frac{1}{aH} \right) = a \int_0^a d \ln a \left(\frac{1}{aH} \right), \quad (2.4)$$

where $1/aH$ is the Hubble radius.

As previously described, the temperature anisotropies of the CMB are small ($\Delta T/T \approx 10^{-5}$). This suggests that all parts of the sky must have been in causal contact to reach thermal equilibrium. The issue is, however, that our Hubble horizon today (defined as the distance which light has traveled since the Big Bang) corresponds to roughly a million causally disconnected regions. This is known as the horizon problem.

2.2.3 The Monopole Problem

Magnetic monopoles are topological defects predicted to arise due to phase transitions around the GUT scale $T \approx 10^{16} \text{ GeV}$ [8]. As the temperature drops below the GUT scale energy, the Higgs field acquires a non-zero vacuum expectation value and the symmetry is spontaneously broken. An analogy can be made with the cooling of a ferromagnet: when the metal cools below the Curie temperature, thermal excitations lose strength and magnetic

dipoles will start aligning with their neighbours. While any direction is initially equi-probable, once a few dipoles have randomly chosen a direction, their neighbours will align themselves accordingly. If the distance between two regions is larger than the particle horizon, then there is no reason to expect that the Higgs field would take the same vacuum expectation value in these regions. The boundary between these two regions is referred to as a topological defect. Again an analogy can be made with dislocations in a ferromagnetic crystal.

Magnetic monopoles are predicted to be stable and it is expected that they were created with a number density comparable with photons [8]. However, for radiations $\rho_\gamma \sim 1/a^4$, while magnetic monopoles are non-relativistic due to their heavy mass so they follow $\rho_{mon} \sim 1/a^3$. This means that the density of photons decreases quicker than the density of monopoles. At some point, it would therefore be expected that monopoles dominate over photons. This is clearly incompatible with the current observations as there is currently no observational evidences for magnetic monopoles except a controversial experiment by Cabrera in 1982 [9].

To illustrate the principle of spontaneously broken symmetries and symmetry restoration, we follow the example in [10]. Let us consider two real scalar fields ϕ and ψ with a potential :

$$V(\phi, \psi) = V_0 - \frac{1}{2}m^2\phi^2 + \frac{1}{4}\lambda_1\phi^4 + \frac{1}{2}\lambda_2\phi^2\psi^2. \quad (2.5)$$

In the case when $\psi = 0$, the fourth term of the potential becomes null and $V(\phi)$ has two minima at $\phi = \pm (m/\sqrt{\lambda_1})$. The minima represent the vacuum expectation values of the field ϕ and the symmetry $\phi \rightarrow -\phi$ is spontaneously broken.

On the other hand, if ψ^2 is homogeneous and time independent, and we as-

sume the effective mass squared of ϕ (the second derivative of the potential with respect to ϕ at the origin) to be positive, then the symmetry is restored since there is a unique minimum at the $\phi = 0$ as shown on the figure below.

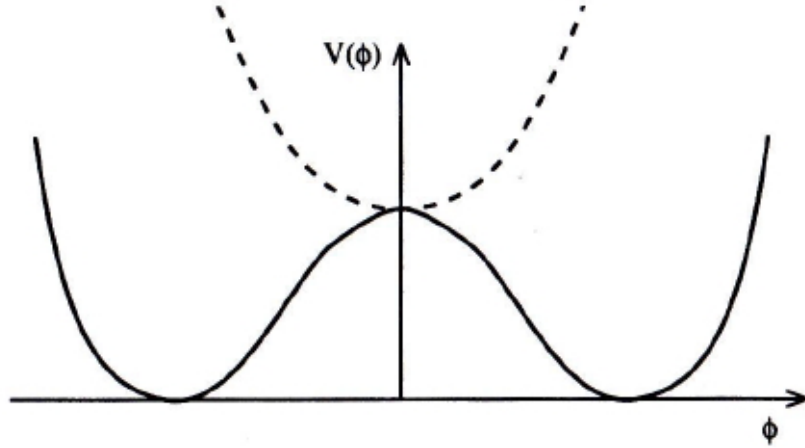


Figure 2.1: The solid line illustrates the potential when $\psi = 0$, while the dashed line shows the potential with $\psi^2 > m^2/\lambda_2$. From [10].

In the case of topological defects, we can form a similar argument where the field ψ depends on the temperature and the symmetry is restored above a critical temperature (this is the Curie Temperature in our analogy with ferromagnets). As the Universe expands, the temperature decreases and at some point becomes smaller than the critical temperature. Right before symmetry breaking, the spatial average of the field ϕ is 0. Yet, because of thermal or quantum fluctuations, different locations in space will have either small positive or negative fluctuations. When the symmetry is broken, and $\psi = 0$, ϕ will roll towards the nearest vacua $\phi = \pm (m/\sqrt{\lambda_1})$ with a topological defect separating regions with different vacua.

2.3 Cosmological Inflation

Cosmological inflation can be defined as a period of accelerated expansion:

$$\ddot{a} > 0. \tag{2.6}$$

Inflation is capable of providing a solution to the issues described above. For example, the condition (2.6) is equivalent to $\frac{d}{dt} \frac{1}{aH} < 0$, which means that, given sufficient expansion, inflation will drive Ω towards 1 according to equation (2.3) regardless of the initial curvature index. Moreover, since $\frac{1}{aH}$ is the co-moving Hubble's length, inflation reduces the size of the observable Universe as shown in figure 2.2 . The idea that the Universe we observe today originated from one small smooth patch solves both the horizon and monopole problems. Indeed, it implies that all parts of the observable sky have been in thermal equilibrium previously, hence explaining the small temperature anisotropies in the Cosmic Microwave Background. Furthermore, since the observable Universe originated as one small patch, the number density of the topological defects has been diluted.

The figure below summarises the main features of inflation and illustrates how inflation can solve the problems we described previously. The accelerated expansion of the Universe during inflation reduces the Hubble horizon as we mentioned that an accelerated expansion is equivalent to $\frac{d}{dt} \frac{1}{aH} < 0$, where $\frac{1}{aH}$ is the Hubble length. After a sufficient number of e-folds, the horizon is fully contained into an initial smooth patch. This is how inflation solves the different problems we described previously. The horizon problem, for example, is resolved since the Universe we observe today originates from a single smooth Hubble patch. After inflation, the condition $\frac{d}{dt} \frac{1}{aH} < 0$ is no longer satisfied and the Hubble horizon starts to expand. The evolution of the Hubble horizon is shown by the blue arrow in the figure below.

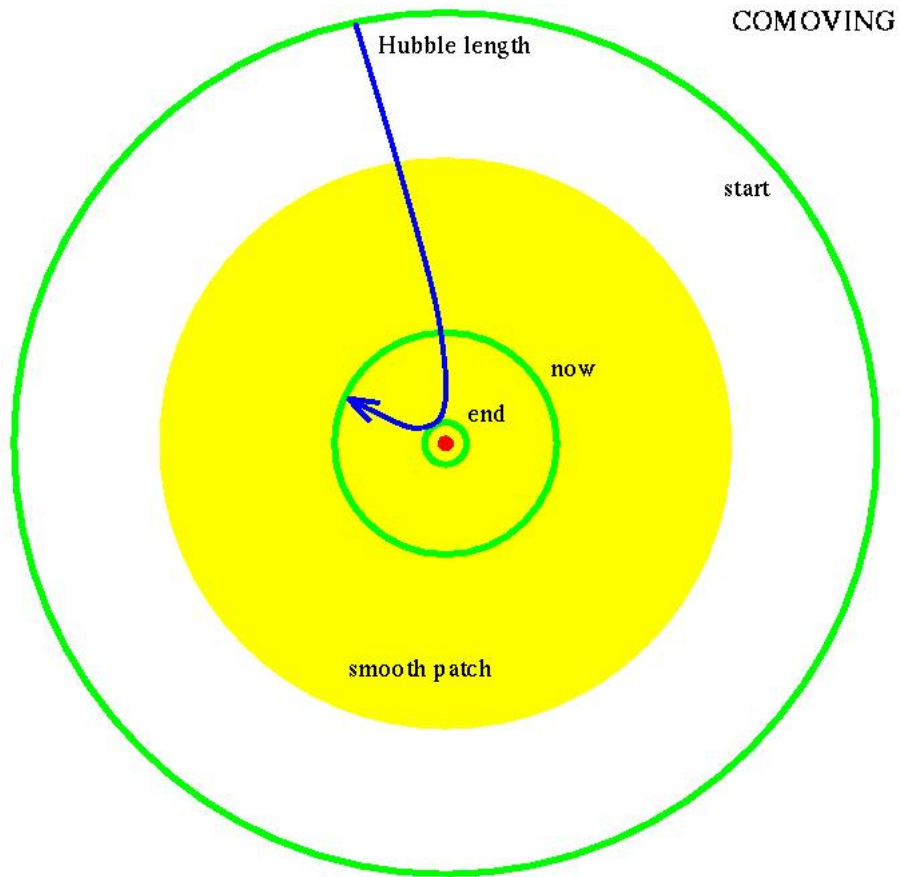


Figure 2.2: Schematic of the inflationary solution to the horizon problem. From [1].

The different parts of the figure are described above.

2.4 Scalar Field Inflation

We reviewed some cosmological problems which can be solved by a period of accelerated expansion at early times. The issue is now to find a new kind of matter whose equation of state satisfies the condition $\ddot{a} > 0$.

Since the Universe is isotropic, its stress-energy-momentum tensor is given by the perfect fluid approximation:

$$T^{\mu\nu} = (p + \rho)u^\mu u^\nu - p\eta^{\mu\nu}, \quad (2.7)$$

where p is the pressure, ρ the density of the Universe, w^μ is the four-velocity vector (with $u^0 = 1$ and $u^i = 0$) and $\eta^{\mu\nu} = \eta_{\mu\nu}^{-1}$ is the inverse of the Minkowski metric with signature $(+, -, -, -)$.

The stress-energy tensor obeys the conservation law : $T_{;\mu}^{\mu\nu} = 0$ which gives the continuity equation:

$$\dot{\rho} = -3H(\rho + p). \quad (2.8)$$

The derivation of this equation is detailed in Appendix 1.

The density and pressure ρ and p are linked through the equation of state: $p = \omega\rho$, where ω is a dimensionless number[11].

Using Friedmann equation (2.1) and (2.8), the condition for inflation (2.6) can be re-expressed as: $\rho + 3p < 0$.

An example of a type of matter with a broken energy dominance ($\rho + 3p < 0$) is a positive cosmological constant for which: $p_\Lambda = -\rho_\Lambda$. The solution of Einstein's equation with this equation of state is a deSitter Universe with $a \propto e^{H_\Lambda t}$ for $t \gg H_\Lambda^{-1}$.

The most common particle candidate to drive inflation is a scalar field known as the inflaton ϕ . Its energy density and pressure are given as : $\rho = \frac{1}{2}\dot{\phi}^2 + V(\phi)$ and $p = \frac{1}{2}\dot{\phi}^2 - V(\phi)$. Spatial derivatives can be neglected as they would be “smoothed” by inflation. Scalar fields are successful candidates if $\dot{\phi}^2 \ll V(\phi)$. In order to determine if a given potential would lead to an inflationary period, it is necessary to study the behavior of the homogeneous classical scalar field in an expanding Universe using the Klein-Gordon equation (2.9) and the Friedmann equation for a homogeneous scalar field (2.10) :

$$\ddot{\phi} + 3H\dot{\phi} + \frac{\partial V}{\partial \phi} = 0 \quad \text{and} \quad (2.9)$$

$$H^2 = \frac{8\pi G}{3} \left(\frac{1}{2} \dot{\phi}^2 + V(\phi) \right). \quad (2.10)$$

For the inflaton, it is possible to neglect the term which contains the spatial derivatives in the Klein-Gordon equation and hence only consider homogeneous scalar fields. This is due to the fact that any gradient will rapidly tend to zero due to the rapid expansion of the Universe during inflation. This can be seen mathematically in the next chapter, where the Klein-Gordon equation is derived.

Chapter 3

Field Fluctuations in a Time Dependent Background

3.1 Inhomogeneous Universe

In the current understanding, the Universe was made nearly flat and homogeneous by an early period of rapid expansion known as inflation. During this period the physical Universe expanded super-luminally thus resulting in a reduction in distance to the horizon. This exponential expansion is the reason why the Universe appears to be uniform and flat today.

Perfect homogeneity, however, is never achieved, at least not on the quantum scale. Quantum fluctuations in an inflationary patch are stretched to classical size. These seed perturbations are believed to have caused inhomogeneities in the early photons, baryons and dark matter fluids which later collapsed into the large-scale structures we observe today and left their imprints on the Cosmic Microwave Background.

3.2 The Klein-Gordon Equation

3.2.1 The Klein-Gordon Equation in Flat Space-Time

Let us consider a scalar field $\phi(\vec{x}, t)$. The action for this scalar field is given by the following equation:

$$S = \int_M d^4x \mathcal{L}(\phi, \partial_\mu \phi), \quad (3.1)$$

where \mathcal{L} is the Lagrangian density and M is a 4-dimensional domain. We use Hamilton's principle by requesting that $\delta S = 0$ when the variations of the field and its derivative are given by:

$$\phi \rightarrow \phi + \delta\phi, \quad \partial_\mu \phi \rightarrow \partial_\mu \phi + \delta\partial_\mu \phi \quad \text{and} \quad \delta\partial_\mu \phi \rightarrow \partial_\mu \delta\phi. \quad (3.2)$$

This gives at first order:

$$\begin{aligned} \delta S &= \int_M d^4x \left\{ \frac{\partial \mathcal{L}}{\partial \phi} \delta\phi + \frac{\partial \mathcal{L}}{\partial (\partial_\mu \phi)} \delta(\partial_\mu \phi) \right\} \\ &= \int_{\partial M} d^3\sigma n_\mu \frac{\delta \mathcal{L}}{\delta (\partial_\mu \phi)} \delta\phi + \int_M d^4x \left\{ \frac{\delta \mathcal{L}}{\delta \phi} - \partial_\mu \frac{\delta \mathcal{L}}{\delta (\partial_\mu \phi)} \right\} \delta\phi, \end{aligned} \quad (3.3)$$

where n^μ is a unit vector oriented normally to the boundary ∂M of M , and $d^3\sigma$ is a 3-dimensional volume element on ∂M . We choose to consider only variations that vanish on ∂M and therefore the first term vanishes. Then, the integrand in the second term must vanish for $\delta S = 0$ to hold for an arbitrary variation of the field $\delta\phi$.

This result gives the Euler-Lagrange equation:

$$\partial_\mu \frac{\partial \mathcal{L}}{\partial (\partial_\mu \phi)} - \frac{\partial \mathcal{L}}{\partial \phi} = 0. \quad (3.4)$$

Let us now consider the Lagrangian for a real scalar field:

$$\mathcal{L} = \frac{1}{2} \partial^\mu \phi \partial_\mu \phi - V(\phi). \quad (3.5)$$

In this case, the Euler-Lagrange equation gives :

$$\square \phi + \frac{\partial V}{\partial \phi} = 0. \quad (3.6)$$

This is the Klein-Gordon equation, where \square is the d'Alembert operator $\square = \partial^\mu \partial_\mu$.

The Klein-Gordon equation is derived in more detail in Appendix 2.

3.2.2 The Klein-Gordon Equation in Curved Space-Time

In curved space time, the action is of the form [1]:

$$S = \int d^4x \sqrt{-g} \mathcal{L}, \quad (3.7)$$

where g is the determinant of the metric $g_{\mu\nu}$ and for the conformally flat FLRW metric:

$$g^{\mu\nu} = a^2 \eta^{\mu\nu}, \quad (3.8)$$

where $\eta^{\mu\nu}$ is the Minkowski metric for which $\sqrt{-\eta} = 1$.

Hence, $\sqrt{-g} = a^3$. The result of using Hamilton's principle on this new action also gives the Euler-Lagrange equation but this time with $\mathcal{L} \rightarrow a^3 \mathcal{L}$.

The Euler-Lagrange equation is :

$$\partial_\mu (a^3 \partial^\mu \phi) + a^3 \frac{\partial V}{\partial \phi} = 0, \quad (3.9)$$

with $\partial^\mu = g^{\mu\nu} \partial_\nu$, where $g^{\mu\nu}$ is the inverse of the metric. This gives the Klein-Gordon equation in curved space-time:

$$\ddot{\phi} - a^{-2} \nabla^2 \phi + 3H\dot{\phi} + \frac{\partial V}{\partial \phi} = 0. \quad (3.10)$$

This form of the Klein-Gordon equation is also derived in more details in Appendix 2.

3.3 Quantum Fluctuations of a Massless Scalar Field

If we consider a massless scalar field $\chi(\vec{x}, t)$ with its small quantum perturbations $\delta\chi(\vec{x}, t)$, we can separate the classical background χ from the perturbation and write the field as:

$$\chi(\vec{x}, t) \rightarrow \chi(t) + \delta\chi(\vec{x}, t). \quad (3.11)$$

In this way, both the field and its perturbation follow the Klein-Gordon equation. In momentum space, let us consider the Fourier transform $\delta\chi_k$ of the perturbation $\delta\chi$.

The standard formula for a Fourier transform is:

$$\delta\chi_k(t) = \int \frac{d^3\vec{x}}{(2\pi)^{3/2}} e^{-i\vec{k}\cdot\vec{x}} \delta\chi(\vec{x}, t). \quad (3.12)$$

In momentum space, using $V(\chi) = 0$, the Klein-Gordon equation (3.10) becomes:

$$\delta\ddot{\chi}_k + 3H\delta\dot{\chi}_k + \frac{k^2}{a^2}\delta\chi_k = 0. \quad (3.13)$$

Using equation (3.13), we will show that the perturbations have a different behaviour depending on the wavelength λ of the perturbation. Two cases must be defined : the infrared case: $k \ll aH$, where the wavelength λ is outside the horizon: $\lambda \gg (aH)^{-1}$, and the ultraviolet: $k \gg aH$, where the wavelength is within the horizon $\lambda \ll (aH)^{-1}$.

In the ultraviolet regime, the friction term $3H\delta\dot{\chi}_k$ can be neglected and equation (3.13) reduces to the harmonic oscillator equation with frequency k^2/a^2 :

$$\delta\ddot{\chi}_k + \frac{k^2}{a^2}\delta\chi_k = 0. \quad (3.14)$$

The frequency is time dependent since the scale factor is a function of time, but qualitatively one can expect the fluctuations to oscillate while the wavelength is within the horizon.

In the infrared regime, $k \ll aH$ and the k^2/a^2 term can be neglected. Then equation (3.13) becomes:

$$\delta\dot{\chi}_k + 3H\delta\chi_k = 0, \quad (3.15)$$

which, since H is effectively constant, has a solution $\delta\chi_k = Ae^{-3Ht} + B$, where A and B are constants of integration. We notice here that the oscillations of the perturbation stop after crossing the horizon.

If we consider the special case where $k = aH$, then all terms must be considered and equation (3.13) may be written as:

$$\delta\ddot{\chi}_k + 3H\dot{\delta\chi}_k + H^2\delta\chi_k = 0, \quad (3.16)$$

and, using the fact that H is constant, we found that the solution is of the form $\delta\chi_k = Ae^{\frac{H}{2}(-3+\sqrt{5})t} + Be^{\frac{H}{2}(-3-\sqrt{5})t}$, where A and B are constants of integration.

The general picture is that given a perturbation with an initial wavelength $\lambda \sim a/k$ inside the horizon, the fluctuations oscillate until the wavelengths become of the order of the horizon at which point, the oscillations stop and the perturbation gets frozen.

We can convert the Klein-Gordon equation into an harmonic oscillator equation, to do this we move to conformal time $d\eta = dt/a$ and use the transformation :

$$\delta\chi_k = \frac{\delta\sigma_k}{a}. \quad (3.17)$$

The Klein-Gordon equation becomes:

$$\delta\sigma_k'' + \left(k^2 - \frac{a''}{a}\right)\delta\sigma_k = 0, \quad (3.18)$$

where $'$ means $\partial/\partial\eta$. We also use a pure deSitter background: $a \sim e^{Ht}$ so $a(\eta) = -\frac{1}{H\eta}$ and $H = \dot{a}/a$ is constant. Equation (3.18) is known as the Mukhanov-Sasaki equation.

On the sub-horizon scale, the k^2 term is dominant ($k^2 \gg \frac{a''}{a} = aH$). The solution is a plane wave:

$$\delta\sigma_k = Ae^{ik\eta} + Be^{-ik\eta} \text{ for } k \gg aH. \quad (3.19)$$

In the ultraviolet regime, the fluctuations oscillate as in flat space-time. The reason is, when the wavelength is much shorter than the horizon scale, the space-time can be approximated as flat.[7]

On super-horizon scale $k^2 \ll \frac{a''}{a}$, the k^2 term can be dropped and a solution may be found by comparing the expression of $(\delta\sigma'_k a)'$ and $(a'\delta\sigma_k)'$. The solution is :

$$\delta\sigma_k = B(k) a \text{ for } k \ll aH, \quad (3.20)$$

where $B(k)$ is a constant of integration. This result shows the freezing of the perturbations once past the horizon.

Chapter 4

Inflaton fluctuations in multi-field scenarios

4.1 Motivations

During inflation, all light scalar fields undergo stochastic fluctuations. Some perturbations are stretched beyond the Hubble length due to the expansion of the Universe and are believed to be the seeds for the formation of large scale structures. Their effects can also be seen in the temperature inhomogeneities in the Cosmic Microwave Background Radiation. In the case of multi-field inflation, the dynamics of the coupled fields can be complicated as the fluctuations of one scalar field may influence the fluctuations of the others [13].

Two articles [14, 15] have recently discussed the dynamics of the fluctuations of flat directions using the stochastic approach. This formalism is described in the following section. These two articles deal with flat and non-flat directions. A flat direction is defined as a direction in field space in which the potential is zero (or constant if there is a zero point constant).

This means that the field can vary at no cost in energy. A similar definition is proposed in [14], where flat directions are configurations where some of the field values are related to each other while the rest are set at zero. A more detailed example is provided in section 4.4.3.

The two articles arrived at different conclusions. In [14], the variance of the fluctuations of the inflaton saturates due to the effect of the non-flat direction unless the coupling between the flat and the non-flat direction is taken to be very small. Conversely, in [15], it is claimed that a non-flat direction cannot block the fluctuations of a coupled flat one since the non-flat direction cannot have large fluctuations itself due to its large mass.

However, it is important to note that these two articles have considered different approaches. In [14], all fields are massless, while in [15] all possible masses are allowed and the authors calculate a zero-point contribution which is subtracted from the correlators. This zero-point contribution accounts for the fact that the noise correlation functions have a non-zero vacuum expectation value. Similarity may be drawn from the idea of vacuum energy, the zero-point contribution represents the stochastic noise which is not due to the small wavelength modes.

In classical slow-roll inflation as described in Chapter 2, it is assumed that the classical fluctuations dominate over the quantum ones. If instead, it is assumed that the quantum fluctuations dominate, one has what is called eternal inflation [1]. Eternal inflationary models suppose that once inflation starts, it carries on forever and creates an indefinitely large volume in which we would be living. However, in the case of eternal inflation, the inflaton quantum fluctuations are the drivers behind the expansion of the Universe, and eternal inflation depends on the ability of the inflaton to have large fluctuations. Since the inflaton is a flat direction of the inflationary potential, it is interesting to see the evolution of its fluctuations in multi-

field scenarios. If the variance of the flat direction saturates as claimed in [14], this result would impair the viability of multi-field eternal inflationary models.

In this chapter, we revisit the stochastic approach introducing what we believe to be the correct mathematical treatment and we compare the results obtained with the previous articles.

4.2 Field Equations and the Stochastic Approach

A process is called stochastic if it is non-deterministic (i.e. if the result of the experiment cannot be used to predict the result which would be obtained if the experiment would be repeated). A popular example could be the flipping of a coin. Obtaining the result “head” does not predict whether the next result will be “head” or “tail”. Since the flipping of a coin is a time-discrete experiment that can only take two values, it is called a Bernoulli process.

In our case, the effect of the momentum modes with a short wavelength (compared to the Hubble horizon) on the modes with long wavelengths is a non-deterministic time-dependent effect which we model as a stochastic process. This is described in more details below.

We consider a potential V with a series of fields ϕ_i and their conjugate momenta π_i . These fields follow the Klein-Gordon equation. In the Hamiltonian picture :

$$\dot{\phi}_i = \pi_i, \quad \dot{\pi}_i + 3H\pi_i - \frac{\nabla^2 \phi_i}{a^2} + \frac{\partial V}{\partial \phi_i} = 0. \quad (4.1)$$

As shown in the previous chapter, the fluctuations of the fields ϕ_i behave

differently depending on whether their wavelengths are smaller or larger than the Hubble horizon . Hence, the fields ϕ_i are separated into two parts : the infrared (IR) Φ_i which represents the fluctuations which have already crossed the horizon: $\lambda < (aH)^{-1}$, and the ultraviolet (UV) φ_i part which represents the fluctuations inside the horizon: $\lambda > (aH)^{-1}$:

$$\phi_i(t, \vec{x}) = \Phi_i(t, \vec{x}) + \varphi_i(t, \vec{x}) \quad , \quad \pi_i(t, \vec{x}) = \Pi_i(t, \vec{x}) + \delta\pi_i(t, \vec{x}) \quad , \quad (4.2)$$

such that:

$$\begin{aligned} \Phi_i(t, \vec{x}) &= \int \frac{d^3k}{(2\pi)^3} \phi_i(t, \vec{k}) W(t, \vec{k}) e^{i\vec{k}\cdot\vec{x}} \quad , \\ \varphi_i(t, \vec{x}) &= \int \frac{d^3k}{(2\pi)^3} \phi_i(t, \vec{k}) [1 - W(t, \vec{k})] e^{i\vec{k}\cdot\vec{x}} \quad , \end{aligned} \quad (4.3)$$

and the analogous equations for the conjugate variables. The function $W(t, \vec{k})$ is the window function that marks the transition between the infrared Φ_i and the ultraviolet φ_i parts. The choice of a relevant window function will be the subject of the next section.

The infrared parts obey the following equations (see Appendix 3):

$$\dot{\Phi}_i = \Pi_i + s_{\phi_i} \quad , \quad \dot{\Pi}_i = -3H\Pi_i - \frac{\partial V(\Phi_i)}{\partial \Phi_i} + s_{\pi_i} \quad , \quad (4.4)$$

where the gradient term have been neglected due to the rapid expansion of the Universe, and where :

$$\begin{aligned}
s_{\phi_i}(t, \vec{x}) &\equiv \int \frac{d^3k}{(2\pi)^3} \phi_i(t, \vec{k}) \dot{W}(t, \vec{k}) e^{i\vec{k}\cdot\vec{x}}, \\
s_{\pi_i}(t, \vec{x}) &\equiv \int \frac{d^3k}{(2\pi)^3} \pi_i(t, \vec{k}) \dot{W}(t, \vec{k}) e^{i\vec{k}\cdot\vec{x}},
\end{aligned} \tag{4.5}$$

are the noise terms. As we show in the previous chapter, the UV modes are described by harmonic oscillators while the oscillations are frozen in the IR when the perturbations cross the horizon. The noise terms correspond to the effect of the UV modes on the IR ones. Since the UV modes evolve rapidly compared to the IR, we can model them as stochastic noise while treating the IR as a classical field.[1, 14].

Equations (4.4) are the Langevin equations for the infrared part. The terms s_{ϕ_i/π_i} are the noise terms accounting for the random “kicks” of the ultraviolet modes onto the infrared ones. Because of its random nature, the stochastic noise follows a Gaussian distribution with mean zero [14]. The variance of noise distribution is defined similarly to [14, 15] as the correlation function of s_{ϕ_i/π_i} :

$$\sigma_{\phi_i/\pi_i}^2 = \langle 0 | s_{\phi_i/\pi_i}(t, \vec{x}) s_{\phi_i/\pi_i}(t', \vec{x}) | 0 \rangle. \tag{4.6}$$

In the numerical calculation, the relevant quantity is the correlation functions between the noise terms integrated over a short interval $[t, t + dt]$. This is due to the discretisation of the equation for the numerical simulations which will be discussed later. The integrated correlations functions are :

$$S_{\phi_i/\pi_i} = \int_t^{t+dt} dt'' \int_{t'}^{t'+dt'} dt''' \sigma_{\phi_i/\pi_i}^2(t'', t'''). \tag{4.7}$$

As explained in [14], equations (4.4) and (4.5) are operator equations and the

terms $\phi_k e^{i\vec{k}\cdot\vec{x}}$ may be written in terms of creation and annihilation operators $\hat{a}_k, \hat{a}_k^\dagger$ as seen in the derivation in Appendix 4 for the case of article [15]. However, with a careful choice of window function, one can ensure that the IR/UV split occurs right after the modes have crossed the horizon. In this condition, s_ϕ and s_π commute with each other. They are treated as classical stochastic forces which we model as random gaussian fields with variance given by equation (4.7).

The physical picture described in [16] relating to the noise terms is that quantum modes leaving the horizon become classical, but their quantum phase freezes as well and its value is random. After the UV modes leave the Hubble scale, they start to contribute to Φ but for an observer inside a Hubble patch, it is not possible to make the distinction between the effect of the UV modes and the random fluctuations of the background.

4.3 The Window Function and the Noise Correlators

The window function is used to decompose the field between its infrared and ultraviolet parts after horizon exit. In both articles [15, 14], the window function compares the inverse Hubble length to the physical momentum of the modes. The window function is written as: $\theta(\epsilon a(t)H - k)$. The parameter ϵ is a constant chosen to be less than 1. In order to keep the calculations and the simulations easier, θ is a Heaviside step function. Because a sharp transition between infrared and ultraviolet is unphysical, the parameter $\epsilon = 0.1$ is chosen to be less than 1 to ensure that the transition to infrared occurs well after horizon crossing. This approximation is valid since we are not interested in the exact spatial correlation of Φ_i .

However, in the case where there are tree-level mass terms: $m_{\Phi_i\Phi_j}^2 \equiv \frac{\partial^2 V}{\partial\Phi_i\partial\Phi_j}$, the relevant quantities for the window function are not only the Hubble length and the momentum but also the masses of the fields. Therefore, the relevant quantity signaling the exit out of the horizon is the physical adiabatic frequency:

$$\omega_i^{(phys)} = \frac{\omega_i(k)}{a} = \frac{1}{a} \sqrt{\vec{k}^2 + m_i^2 a^2}, \quad (4.8)$$

and the window function becomes:

$$W(t, \vec{k}) = \theta(\epsilon H a - \omega_i(k)). \quad (4.9)$$

Using this window function, the integrated noise correlators were imposed as :

$$\begin{aligned} S_{\phi_i} &= \left(\frac{H}{2\pi}\right)^2 dN j_0 \left(a\sqrt{\epsilon^2 H^2 - m_i^2} r\right) \frac{\pi}{2} \left(\epsilon^2 - \frac{m_i^2}{H^2}\right)^{\frac{3}{2}} \\ &\times \theta\left(\epsilon^2 - \frac{m_i^2}{H^2}\right) \left| H_\nu^1 \left(\sqrt{\epsilon^2 - \frac{m_i^2}{H^2}}\right) \right|^2, \end{aligned} \quad (4.10)$$

$$\begin{aligned} S_{\pi_i} &= \left(\frac{H}{2\pi}\right)^2 dN j_0 \left(a\sqrt{\epsilon^2 H^2 - m_i^2} r\right) \frac{\pi}{2} \left(\epsilon^2 - \frac{m_i^2}{H^2}\right)^{\frac{3}{2}} \theta\left(\epsilon^2 - \frac{m_i^2}{H^2}\right) \\ &\times \left| \left(\frac{3}{2} - \nu\right) H_\nu^1 \left(\sqrt{\epsilon^2 - \frac{m_i^2}{H^2}}\right) + \sqrt{\epsilon^2 - \frac{m_i^2}{H^2}} H_{\nu-1}^1 \left(\sqrt{\epsilon^2 - \frac{m_i^2}{H^2}}\right) \right|^2, \end{aligned} \quad (4.11)$$

where : $H_\nu^1(x)$ is the Hankel function of the first kind , $j_0(x)$ is the zeroth order spherical Bessel function, $r = |\vec{x}_1 - \vec{x}_2|$ and $\nu = \sqrt{\frac{9}{4} - \frac{m_i^2}{H^2}}$. $dN = H dt$ is

the increment of number of e-folds.¹

Since we are only interested in the dynamics of the infrared fields in their domains of size $\sim H^{-3}$ and not in different uncorrelated domains, we take $r = 0$ and therefore drop the Bessel function since $j_0(0) = 1$. Furthermore, since we imposed the condition : $\frac{m_i^2}{H^2} < \epsilon^2 < 1$ when we defined the window function in equation (4.9), ν is always a real number while the authors in [15] also consider the case when ν is complex.

In [15], the authors argue that little is known on whether the zero-point fluctuation should be subtracted in the calculation of S_{ϕ_i/π_i} . They show that the zero-point fluctuation is negligible as long as the masses considered are small. However, in the case where $m_i \gg H$, they find that the zero-point fluctuation dominates the noise terms. This problem is solved when the correct window function is used as large masses are not allowed. The physical argument is: if a field has a heavy mass, larger than the Hubble rate, it will never be able to exit the horizon, since the crossing of the horizon happens when the adiabatic frequency (4.8) becomes less than the Hubble rate.

4.4 Numerical Analysis

In this section, the field equations are written in a suitable form to be inputted into the numerical simulations. We present the potential considered and discuss the results of the numerical simulations.

4.4.1 Setup

Following the example of [14, 15], the variables are rescaled to form dimensionless quantities. The fields, the potential and the noise terms (4.10) and

¹Equations (4.10) and (4.11) were derived by Dr Anupam Mazumdar. For a similar calculation in the case of [15], see Appendix 4.

(4.11) become:

$$\begin{aligned}
\Phi_i &\rightarrow \tilde{\Phi}_i = \frac{\Phi_i}{H}, \\
\Pi_i &\rightarrow \tilde{\Pi}_i = \frac{\Pi_i}{H^2}, \\
S_\phi &\rightarrow \tilde{S}_\phi = \frac{S_\phi}{H^2}, \\
S_\pi &\rightarrow \tilde{S}_\pi = \frac{S_\pi}{H^2}, \\
V(\Phi_i) &\rightarrow \tilde{V}(\tilde{\Phi}_i) = \frac{V(\Phi_i)}{H^4}.
\end{aligned} \tag{4.12}$$

For example, in natural units, the field Φ has dimension of energy, while H has dimension $1/time$, which in natural units, is expressed as energy. The ratio $\tilde{\Phi}_i = \frac{\Phi_i}{H}$, is therefore dimensionless.

The Langevin equations can now be expressed in terms of dimensionless variables :

$$\begin{aligned}
\tilde{\Phi}'_i(N) &= \tilde{\Pi}_i(N) + \tilde{s}_{\phi_i}, \\
\tilde{\Pi}'_i(N) &= -3H\tilde{\Pi}_i(N) - \frac{\partial \tilde{V}(\Phi_i)}{\partial \Phi_i} + \tilde{s}_{\pi_i}.
\end{aligned} \tag{4.13}$$

where ' stands for $\frac{d}{dN}$ derivative with respect to the number of e-folds : $N = \int H dt$.

In order to solve these equations numerically, the fields must be discretised by choosing a small “time” step: $dN \ll 1$. For clarity of notation we will also drop the tildes in these equations. The discretised iterative dimensionless Langevin equations are :

$$\begin{aligned}
\Phi_i(N + dN) &= \Phi_i(N) + \Pi_i(N) dN + S_{\phi_i}, \\
\Pi_i(N + dN) &= \Pi_i(N) - 3\Pi_i(N) dN - \frac{\partial V}{\partial \Phi_i} dN + S_{\pi_i}.
\end{aligned}
\tag{4.14}$$

4.4.2 Numerical Simulations

The goal of this project is to design a computer program capable of solving the coupled Langevin equations in order to determine the evolution of the inflationary flat direction. The program created uses C++ and is based on LATTICEEASY [18]. LATTICEEASY is a lattice simulation capable of calculating the evolution of interacting scalar fields in an expanding Universe. Since our equations have no space dependence, a lattice simulation is not required. Besides, such a simulation in deSitter space would require too much computing power. Instead, our program uses the lattice as an array where it can independently solve the equations of motion at each grid points in order to quickly obtain good statistics. This method requires all variables to be defined as arrays but we found that it was to most efficient way to carry out the simulation as it minimises the necessary CPU time. All results are then averaged over the grid.

While the program developed has only kept the basic structure of LATTICEEASY, its “code-skeleton” includes the possibility to run in parallel. This is an attractive feature from LATTICEEASY which means the program can be used in a computing cluster to get even higher statistics if required.

In order to compute the Hankel functions in the noise correlators (4.10) and (4.11), we use the same approximation as [15]:

$$|H_\nu^1(\epsilon)|^2 \simeq \frac{2^{2\nu} \Gamma(\nu)^2}{\pi^2} \epsilon^{-2\nu}.
\tag{4.15}$$

This approximation allows us to restrain from using the third-parties Boost libraries since Hankel functions are not defined as standard functions in C++11.

4.4.3 Numerical Analysis

For our purpose, we have chosen a simpler potential than [14, 15]. This potential is :

$$V = \frac{1}{2}\lambda^2\phi^2\chi^2 + \frac{1}{2}g^2\chi^4 + \frac{\phi^6}{M_{pl}^2}, \quad (4.16)$$

where λ and g are coupling constants, $M_{pl} \simeq 2.4 \times 10^{18} GeV$ is the reduced Planck mass, ϕ is the flat direction and χ is the non-flat one. We found that reducing the number of non-flat directions in the potential compared to [14, 15] has no impact on the dynamics. As previously mentioned, we have also reproduced the results presented in both articles when using their respective treatments for the noise terms and their potential. These results will be shown in the next section.

It is important to note, however, that when the variables are rescaled to dimensionless quantities as shown in (4.12), the term of the form $\frac{\phi^6}{M_{pl}^2}$ becomes $\frac{H^2}{M_{pl}^2}\tilde{\phi}^6$. The ratio $\frac{H^2}{M_{pl}^2}$ can be chosen by setting the tensor to scalar ratio which is estimated from the calculation of the spectrum of the curvature perturbation using the Cosmic Microwave Background data [1]. According to [1], the tensor spectrum is given by:

$$P_h(k) = \frac{8}{M_{pl}^2} \left(\frac{H}{2\pi} \right)^2. \quad (4.17)$$

This relation will permit to give an estimation of the value of $\frac{H}{M_{pl}}$ during inflation using the experimental limits on the tensor to scalar ratio from the

observation of the Cosmic Microwave Background. The prospective detection of gravitational waves will, in the future, permit more accurate estimations of this ratio [17]. For our simulations, it was imposed that : $\frac{H^2}{M_{pl}^2} \sim 10^{-10}$.

The graphic below is a 3D plot of the potential which illustrates the fact that ϕ is indeed almost a flat direction of the potential. We recall the definition that a flat direction is a direction in field-space where the potential is zero (or constant if there is zero-term : i.e. $V = V_0 + \dots$). In the picture, it can be seen that the direction ϕ is indeed almost constant while the value of the potential rises in the χ -direction.

If we use the second definition proposed in 4.1 and [14], setting the χ field to 0 gives $V \sim \phi^6/M_{pl}^2$ which is called a non-renormalisable term in [14]. (This is because the motivation of the potential in [14] comes from Supersymmetry, which is beyond the scope of this study). The purpose of the non-renormalisable term is to lift the flat direction. When ϕ is small compared to the Planck mass this term is suppressed due to its small coupling and ϕ behaves as a flat direction. On the other hand, when the non-renormalisable term becomes large enough, the potential is no longer 0 in the ϕ direction and the flat direction has then been lifted.

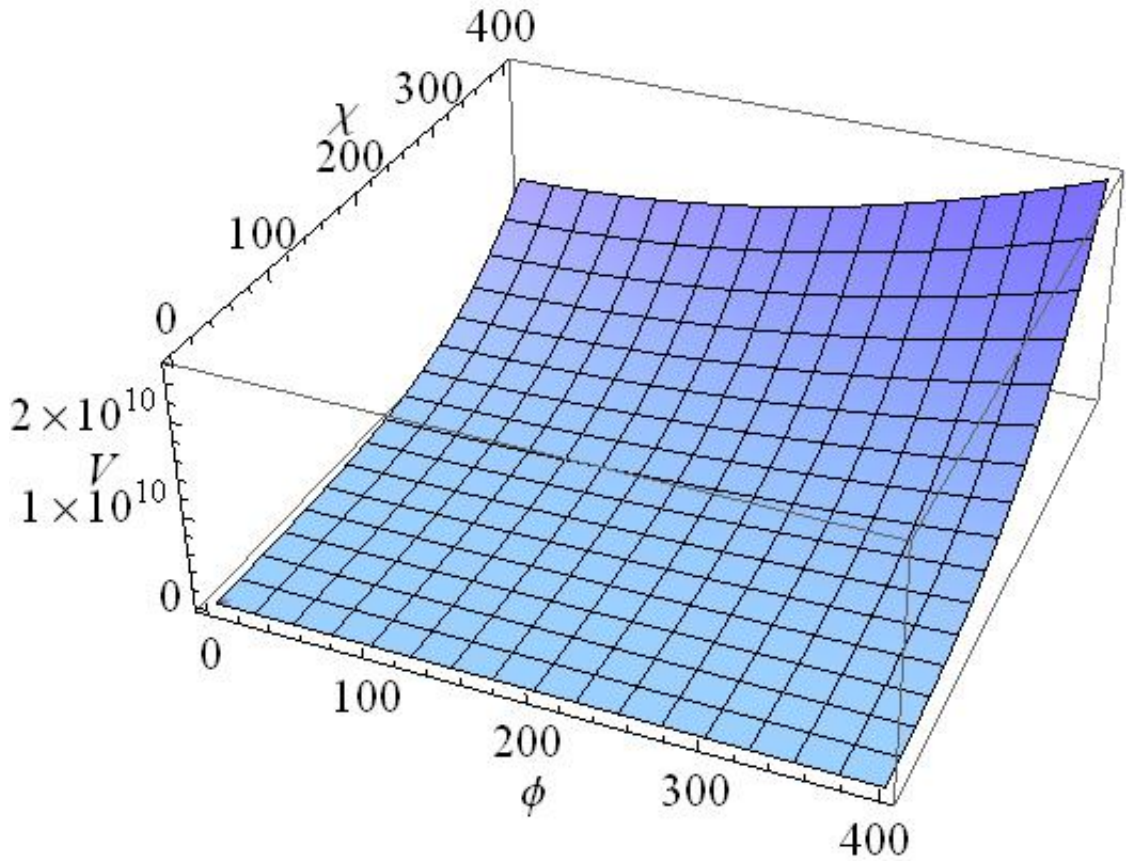


Figure 4.1: The potential shown in equation 4.16 (All variables are dimensionless, as detailed in (4.12).)

4.4.4 Preliminary results

In this section, we prove the viability of the program we developed by reproducing the results obtained in [14, 15] using their potential and respective treatments of the noise correlators. Since our aim in this section is only to reproduce the results of these previous studies and show the validity of our program, we use the same parameters as both articles: the iteration step $dN = 10^{-2}$ and $\epsilon = 0.1$. In order to generate the random numbers, we use the standard C++11 Mersenne-Twister engine “mt19937” similarly to [15]. The potential used by both articles is :

$$V = \frac{1}{2}\lambda_e^2 (\Phi^2 + J^2) E^2 + \frac{1}{8}g_1^2 J^4 + \frac{1}{8}g_2^2 (J^4 + 4E^4 - 4J^2 E^2) + \frac{H^2}{M_{pl}^2} \Phi^6, \quad (4.18)$$

where Φ is the flat direction of the potential, J, E are two non-flat directions, M_p is the reduced Planck mass and λ_e, g_1, g_2 are coupling constants. In this example, we follow [14, 15] and put all coupling constants to 1. The potential then becomes :

$$V = \frac{1}{2}\Phi^2 E^2 + \frac{1}{2}E^4 + \frac{1}{4}J^4 + \frac{H^2}{M_{pl}^2} \Phi^6. \quad (4.19)$$

The initial conditions for both articles are: $\Phi(0) = E(0) = J(0) = 0$.

In the case of [14], all fields have no effective masses and the noise correlators are also constant with values :

$$S^\phi = (1 + \epsilon^3) \frac{dN}{4\pi^2}, \quad S^\pi = \epsilon^4 \frac{dN}{4\pi^2}. \quad (4.20)$$

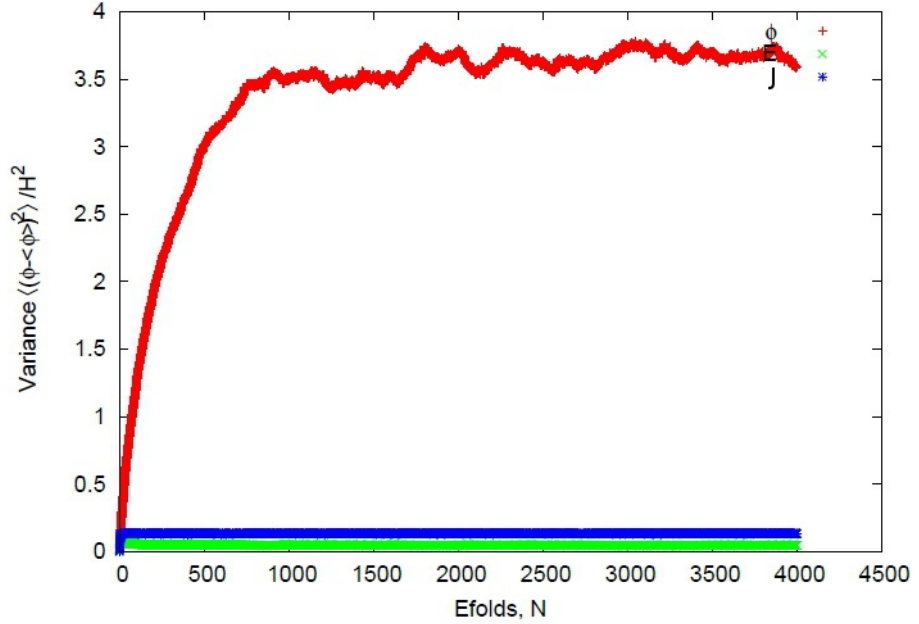


Figure 4.2: Time evolution of the flat and non-flat directions according to [14]

Similarly to [14], we found that the variance of the flat-direction Φ saturates around $3.5H^2$ after about a thousand e-folds, while the variances of the non-flat directions stay close to zero.

In the case of [15], the effective masses of the fields are given as:

$$\frac{m_{\Phi_i}^2}{H^2} = \frac{\partial^2 V(\Phi_i)}{\partial \Phi_i^2}, \quad (4.21)$$

since the authors of [15] have decided to neglect the non diagonal terms. Hence:

$$\frac{m_{\Phi}^2}{H^2} = E^2 + 30\frac{H^2}{M_{pl}^2}\Phi^4, \quad \frac{m_E^2}{H^2} = \Phi^2 + 6E^2, \quad \frac{m_J^2}{H^2} = 3J^2. \quad (4.22)$$

The non-diagonal terms of the mass matrix have been neglected. The noise correlators are functions of the fields masses, the approximation of the Hankel functions (4.15) is not the same for different mass ranges. The complete expressions for the noise correlators are given in [15].

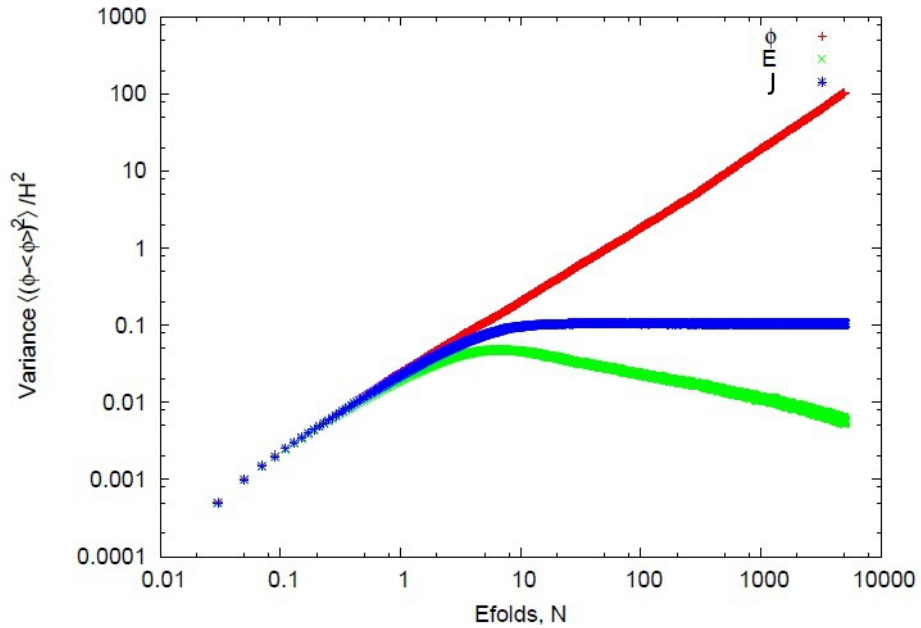


Figure 4.3: Time evolution of the flat and non-flat directions according to [15]

Similarly to [15], we found that the variances of the fields are initially degenerate but the variance of the flat direction Φ does not saturate within 4000 e-folds as is the case in [14]. The variance of the J field (blue line) saturates at small value: this stabilisation is explained by the fact that the mass of the J field only depends on the value of the field J when the coupling constants are all equal to 1. We found:

$$\frac{m_J^2}{H^2} = 3J^2. \quad (4.23)$$

In the case of the E field, its mass depends on both Φ and E , the expression is :

$$\frac{m_E^2}{H^2} = \Phi^2(N) + 6E^2(N). \quad (4.24)$$

Since the Φ field is allowed to have large fluctuations, it can take large values which means that the mass of the E field becomes larger. Massive fields fluctuate at a higher cost in energy, hence the variance of the E field is dropping.

4.4.5 Numerical Results

In the previous section, it was shown that our program, given the same input, is able to reproduce the results shown in [14, 15]. In this section, we present the time evolution of the variances of the infrared modes using the formalism we introduced in this work. We decided to run our program with the same parameters as the articles presented in the section above. Therefore we take $dN = 0.01$ for a time step, $\epsilon = 0.1$ and we choose for initial

conditions : $\Phi_i = \Pi_i = 0$ as in [14, 15]. Due to the grid of the program, the number of independent runs must be a cubed-root integer and we chose $22^3 = 10648$ while each run goes up to 4000 e-folds.

We recall that the potential we used for this simulation is slightly different than [14, 15] since we neglected the J field. This field has no coupling term with the Φ and E fields in the case of [14, 15] and hence acts as a spectator non-flat direction, it can therefore be removed without loss of generality. The potential we use in this section is :

$$V = \frac{1}{2}\lambda^2\Phi^2\chi^2 + \frac{1}{2}g^2\chi^4 + \frac{H^2}{M_{pl}^2}\Phi^6, \quad (4.25)$$

where Φ is the flat direction, χ the non-flat and λ, g are constants equal to 1.

In the following Figure 4.4, we show the results for a constant coupling $\lambda = 1$ and for $\frac{H^2}{M_{pl}^2} = 10^{-10}$. The red line represents the evolution of the flat direction , the green line is for the non-flat direction.

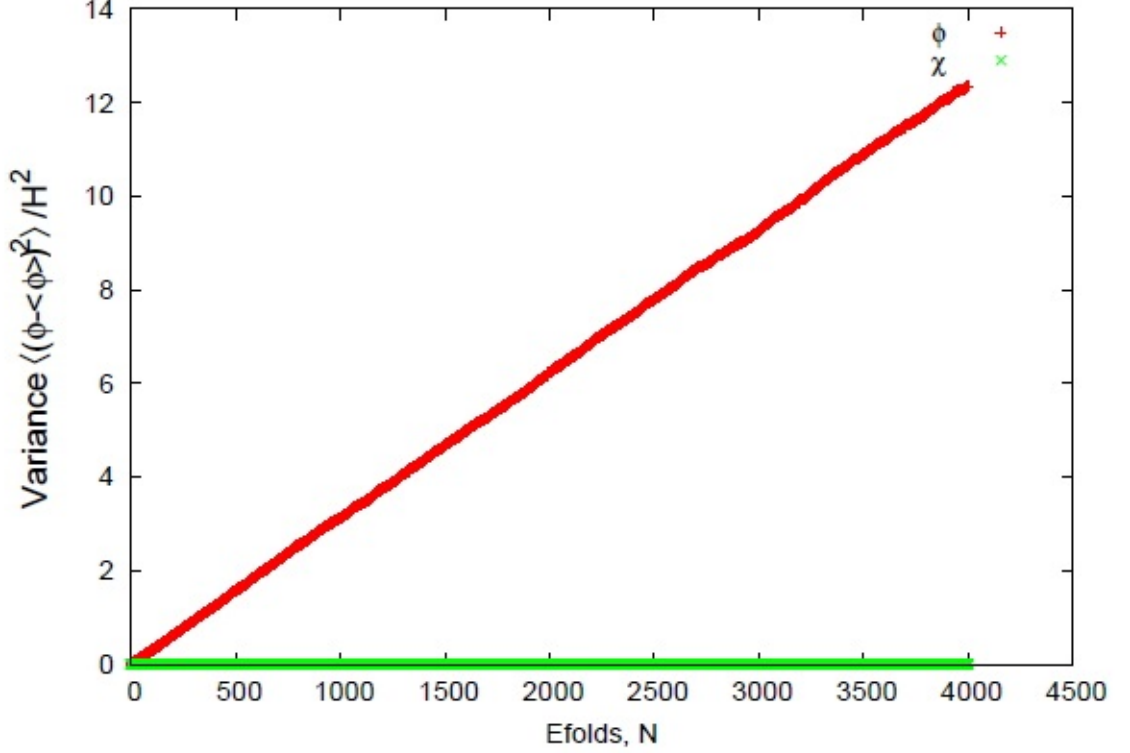


Figure 4.4: Evolution of the variances of the infrared modes for $\lambda = g = 1$ and $\frac{H^2}{M_{pl}^2} = 10^{-10}$.

The results are clearly in agreement with [15] since the variance of the flat direction does not saturate. The value of the variance, however, is much lower than what is found in [15]. We explain this discrepancy using the fact that our window functions are different. Since our definition of the infrared modes is more selective than the one used in [15, 14], there are fewer modes whose fluctuations contribute to the infrared variance. This graphic also shows that the simulation done in [14] is only valid in the special case considered in their articles where the fields are massless. We should therefore concentrate our efforts on comparing our study with [15].

Evolution of the masses

In this section, we discuss the evolution of the coupling masses of each fields. While this is not discussed in [15], it is interesting to comment on this re-

sult as it gives us some insight on the behaviour of the two directions. The masses are averaged over the number of independent runs as a function of the number of e-folds. The masses of the two fields are given by:

$$\begin{aligned}\frac{m_{\Phi}^2}{H^2} &= \lambda^2\chi^2 + 30\frac{H^2}{M_{pl}^2}\Phi^4, \\ \frac{m_{\chi}^2}{H^2} &= \lambda^2\Phi^2 + 6g^2\chi^2.\end{aligned}\tag{4.26}$$

Similarly to [15], the non-diagonal terms in the mass matrix (4.21) have been neglected. Φ and χ are not mass-eigenstate fields (their mass matrix is not diagonalised : $\frac{\partial^2 V}{\partial\Phi\partial\chi} = 2\Phi\chi$), instead their noise matrix is diagonal (there is no term involving cross-correlation). If the simulation had been performed for mass-eigenstate fields obtained by diagonalising the mass matrix, then the noise matrix for these fields would not be diagonalised. This would complicate the equations further so for simplicity, it was decided to ignore the cross-terms of the mass matrix.

Below is shown the evolution of the averaged mass squared for the fields Φ and χ . In the case of the Φ field, the dominant term is $\lambda^2\chi^2$ because we chose $\lambda = 1$ while the ratio $\frac{H^2}{M_{pl}^2}$ has a small value. The variance of the χ field, however, is small so the field cannot take values far from its original value which is zero. The Φ field is therefore free to fluctuate and hence takes large values. Since both coupling are taken as $\lambda = g = 1$, the term $\lambda^2\Phi^2$ becomes the dominant term in the expression of $\frac{m_{\chi}^2}{H^2}$. The χ field developed a large mass and is further barred from fluctuating. This feeds into the mass of the Φ field and accentuates the phenomenon further.

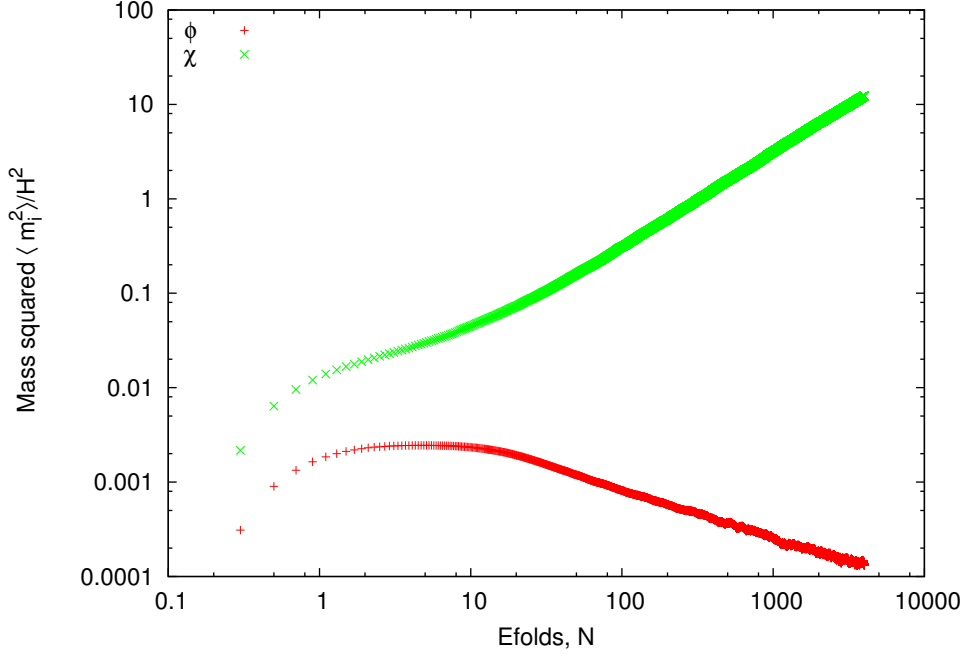


Figure 4.5: Evolution of the masses of the flat Φ and non-flat χ directions for $\lambda = 1$ and $\frac{H^2}{M_{pl}^2} = 10^{-10}$.

Evolution of the variances for the noise correlation functions

In this section we look at the evolution of noise correlation functions and contrast our results with [15]. The choice of a new window function (4.9) which depends on the adiabatic frequency and not only on the momentum means that, compared to [15], it is not necessary to modify the approximations of the Hankel function depending on the mass of the fields. With this setup, the results differ from [15].

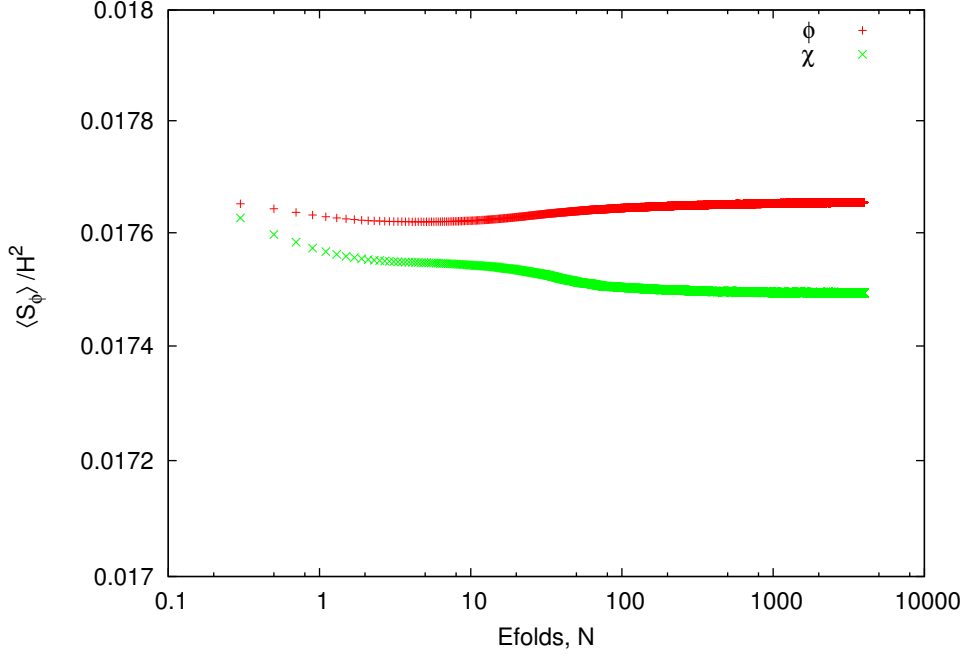


Figure 4.6: Integrated noise correlation function $\langle S_\phi \rangle$ averaged over the number of runs.

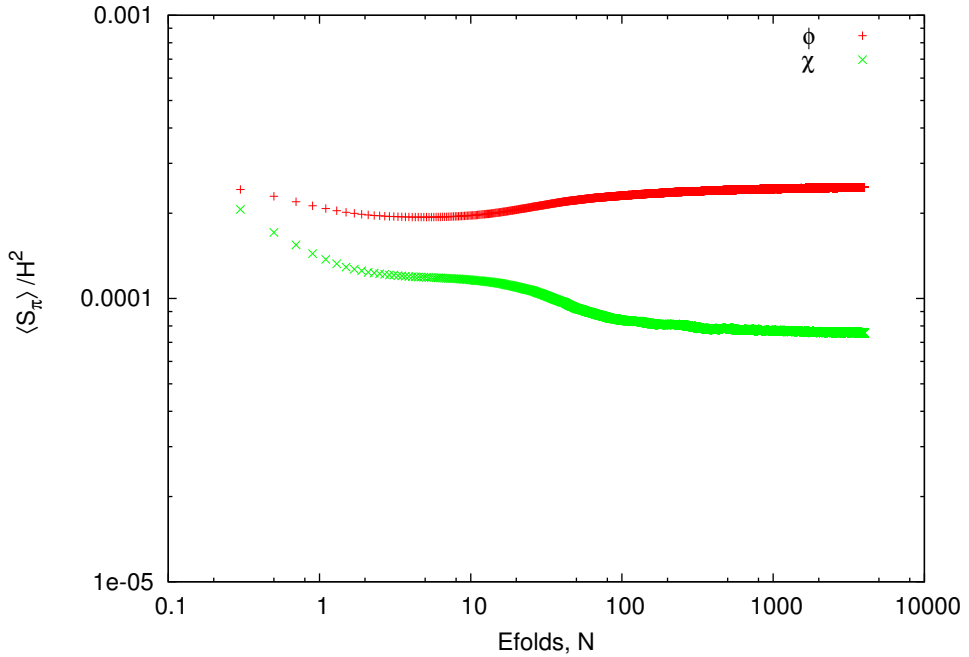


Figure 4.7: Integrated noise correlation function $\langle S_\pi \rangle$ averaged over the number of runs.

Similarly as the masses, S_ϕ and S_π (see (4.10) and (4.11)) have been averaged over the number of independent runs as a function of the number of e-folds.

As in [15], we find $\langle S_\pi \rangle$ has little effect on the calculation since $\langle S_\pi \rangle \ll \langle S_\phi \rangle$. In the case of the field Φ , $\langle S_\phi \rangle$ is mostly constant, this result is consistent with Figure 4.4 since there is no observable change in the rate at which the variance of the field Φ evolves. For the χ field, we do not observe the same rapid decrease as observed in [15]. This difference is once again due to the fact that we use a window function (4.9) compared to [15]. In [15], the variance of the Φ field increases by roughly five orders of magnitude and the field can take large values. The noise correlation functions depend on the mass of the fields and the mass of the χ field depends on the value of Φ . Since in our treatment of the stochastic noise, the variance of the fields is more constrained than in [15], the other variables are also constrained from varying on a large scale.

The value of $\frac{H^2}{M_{pl}^2}$

According to [14], the non-renormalisable term plays no role in the saturation of the variance of the flat direction since the fluctuations never exceed a few units of H . Our results disagree on this particular point. We found that choosing a different value for the ratio $\frac{H^2}{M_{pl}^2}$ has a drastic impact on the results and that the variance of the flat direction may, in that case, reach a stationary limit. The following figure shows the evolution of the flat direction for different values of $\frac{H^2}{M_{pl}^2}$.

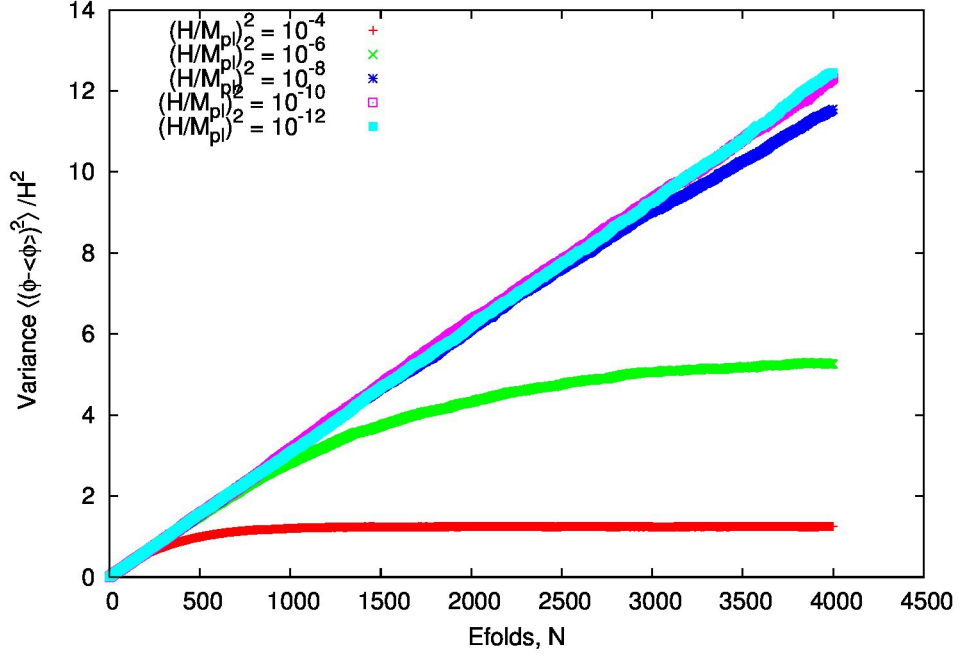


Figure 4.8: Evolution of the variance of the flat direction Φ for $\lambda = 1$ and varying $\frac{H^2}{M_{pl}^2}$.

As it can be seen in Figure 4.8, the saturation of the variance of the flat direction depends on the value of $\frac{H^2}{M_{pl}^2}$ and the effect of the non-renormalisable term. This Figure illustrates the lifting of the flat-direction by the non-renormalisable term $\frac{H^2}{M_{pl}^2} \Phi^6$ as described in 4.4.3: initially the non-renormalisable term is suppressed due to its small coupling but as Φ takes larger values, the non-normalisable term is no longer negligible and the potential is non-zero in the Φ direction.

As described in 4.4.3, the approximation $\frac{H^2}{M_{pl}^2} \sim 10^{-10}$ is obtained from the tensor to scalar ratio. We find that for $\frac{H^2}{M_{pl}^2}$ larger than 10^{-8} , the coupling λ has little effect on the dynamics of the flat direction over the range of e-folds considered. In the case when $\frac{H^2}{M_{pl}^2} = 0$, which is equivalent to removing this term from the potential, the variance of the flat direction grows linearly as shown in Figure 4.9 below. In this situation, only the fluctuations of the non-flat direction can block those of the flat direction and saturate its variance, but as shown in the figure this is not the case. We can therefore conclude

from this figure that the mechanism described in [14] is not sufficient to affect the variance of the flat direction within 4000 e-folds.

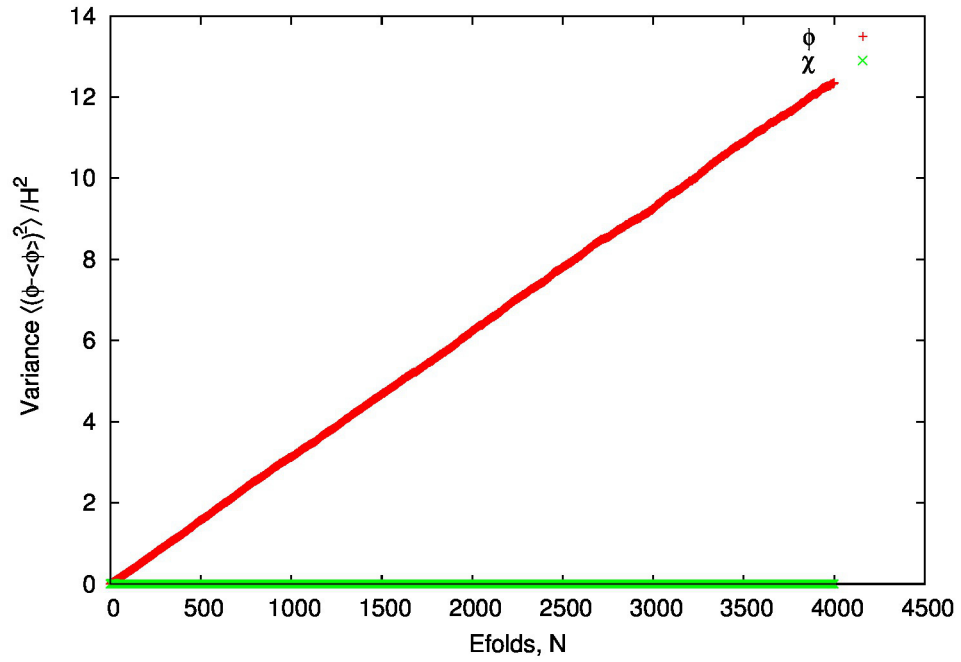


Figure 4.9: Evolution of the variance of the flat Φ and non-flat χ directions for $\lambda = 1$ and $\frac{H^2}{M_{pl}^2} = 0$.

Chapter 5

Conclusion

In this study, we have analysed the time evolution of a flat and a coupled non-flat direction governed by stochastic Langevin equations during inflation. The basic ideas and equations in inflationary cosmology have been reviewed as well as primordial perturbations.

During inflation, all scalar fields fluctuate. In the case of a single field potential, the dynamics of the inflaton are well known. In a multi-field scenario, the coupling of the fields can lead to back-reactions between the fluctuations of each field and this complicated situation requires computer simulations in order to be solved. Previous studies have analysed the evolution of a flat direction in multi-field scenarios either in a special case or in a set-up which is believed to be incomplete.

We have revisited this topic, taking into account the effective masses of the fields for the evaluation of the noise terms. Our definition of a more adequate window function, based on the adiabatic frequency rather than only the momentum of the modes, has solved the dilemma encountered by [15] on whether a zero-point fluctuation should be subtracted. Indeed, [15] found very different results at large masses depending on whether the zero-point fluctuations were included. In our formalism, the noise correlators (and

their zero-point contributions) are zero for large masses when the zero-point fluctuations have a noticeable effect. It is not clear, however, whether the zero-point fluctuations should be included at all.

Regarding the disagreement between [14] and [15] on the behaviour of the flat direction, we found that a coupled non-flat direction cannot acquire an effective mass too large to have fluctuations significant enough to block the fluctuations of the flat direction. The variance of the flat direction then evolves linearly and is proportional to the number of e-folds. However, by making the definition of the IR modes more selective, the fluctuations of the flat direction grow more slowly than in [15].

Eternal inflation assumes that the inflaton is a flat direction of the inflationary potential and requires that its fluctuations can have a large amplitude in order to drive inflation. The results found in [14] meant that eternal inflation would not be a viable model. Whereas our results are more in favour of eternal inflation, we have found a limited growth of the flat direction's fluctuations compared to [15] which raises the question whether the amplitude of these fluctuations would be sufficient to sustain eternal inflation.

Bibliography

- [1] Liddle A. and Lyth D., *The primordial density perturbation*, Cambridge University Press, 2009.
- [2] Hubble E., A relation between distance and radial velocity among extra-galactic nebulae, *Proc. N.A.S.*, 15:168-173,1929.
- [3] Liddle A., An introduction to cosmological inflation, *arXiv:astro-ph/9901124*, 1999.
- [4] Planck Collaboration, Planck 2013 results. XVI. Cosmological parameters, *arXiv:1303.5076*, 2013.
- [5] Bond J., et. al., *The Cosmic Microwave Background & Inflation, Then & Now*, *arXiv:astro-ph/0210007*, 2002.
- [6] Liddle A., *An Introduction to Modern Cosmology*, 2nd edition, Wiley, 2008.
- [7] Riotto A., *Inflation and the Theory of Cosmological Perturbations*, *arXiv:hep-ph/0210162*, 2002.
- [8] Perkins D., *Particle Astrophysics*, 2nd edition, Oxford University Press, 2009.
- [9] Cabrera B., First Results from a Superconductive Detector for Moving Magnetic Monopoles, *Phys. Rev. Lett.* 48, 1378, 1982.

- [10] Liddle A., Lyth D, *Cosmological Inflation and Large-Scale Structure*, Cambridge University Press, 2006.
- [11] Ryden B., *Introduction to Cosmology*, Addison-Wesley, 2003.
- [12] Baumann D., *TASI Lectures on Inflation*, arXiv:0907.5424 , 2012.
- [13] Sanchez J., Enqvist K., *On the fate of coupled flat directions during inflation*, arXiv:1210.7007, 2013.
- [14] Enqvist K., Figueroa D., Rigopoulos G., *Fluctuations along supersymmetric flat directions during Inflation*, arXiv:1109.3024, 2011.
- [15] Kawasaki M., Takesako T., *Stochastic Approach to Flat Direction during Inflation*, arXiv:1207.1165, 2012.
- [16] D. Podolsky, *Inflationary Perturbation: lecture notes*, University of Helsinki, Spring2008.
- [17] Dodelson S., *Modern Cosmology*, Academic Press, 2003.
- [18] Felder G., Tkachev I., *LATTICEEASY: A Program for Lattice Simulations of Scalar Fields in an Expanding Universe*, arXiv:0011159, 2000.
- [19] Islam J. N., *An Introduction to Mathematical Cosmology*, Cambridge University Press, 2002.
- [20] Abramowitz M., Stegun J., *Handbook of Mathematical Functions with Formulas, Graphs, and Mathematical Tables.*, Dover Publications, 1964.

Appendix

Appendix 1: The Equation of Continuity

In this section we derive the equation of continuity (2.8) which relates the density and pressure in the Universe.

We start with the energy momentum tensor

$$T_{\nu}^{\mu} = \text{diag}(\rho, -p, -p, -p). \quad (1)$$

The conservation law $T_{\nu;\mu}^{\mu} = 0$ is satisfied and the covariant derivative is defined as $T_{\nu;\mu}^{\mu} = \frac{\partial T_{\nu}^{\mu}}{\partial x^{\mu}} + \Gamma_{\alpha\mu}^{\mu} T_{\nu}^{\alpha} - \Gamma_{\nu\mu}^{\alpha} T_{\alpha}^{\mu}$,

where Γ_{kl}^i is a Christoffel symbol defined as $\Gamma_{kl}^i = \frac{1}{2}g^{im} \left(\frac{\partial g_{mk}}{\partial x^l} + \frac{\partial g_{ml}}{\partial x^k} - \frac{\partial g_{kl}}{\partial x^m} \right)$, and where g^{im} is the FRLW metric.

For $\nu = 0$, the conservation law gives

$$\frac{\partial T_0^0}{\partial x^0} + \Gamma_{0\mu}^{\mu} T_0^0 - \Gamma_{0\mu}^{\alpha} T_{\alpha}^{\mu} = 0. \quad (2)$$

The relevant non-zero Christoffel symbols are (from [19])

$$\Gamma_{01}^1 = \Gamma_{02}^2 = \Gamma_{03}^3 = \frac{\dot{a}}{a} = H. \quad (3)$$

Finally, we now substitute the Christoffel symbols into (2) and obtain the continuity equation

$$\dot{\rho} + 3H(p + \rho) = 0. \quad (4)$$

Appendix 2: The Klein-Gordon Equation

In this section, we derive the Klein-Gordon equation in flat and curved space-time using the Euler-Lagrange equation which was derived in 3.2.

We start from the Euler-Lagrange Equation obtained previously (3.4)

$$\partial_\mu \frac{\partial \mathcal{L}}{\partial (\partial_\mu \phi)} - \frac{\partial \mathcal{L}}{\partial \phi} = 0, \quad (5)$$

we take the Lagrangian density for a real scalar field

$$\mathcal{L} = \frac{1}{2} \partial^\mu \phi \partial_\mu \phi - V(\phi). \quad (6)$$

Then we compute each term of the Euler-Lagrange equation and find

$$\frac{\partial \mathcal{L}}{\partial (\partial_\mu \phi)} = \partial^\mu \phi, \quad (7)$$

and

$$\frac{\partial \mathcal{L}}{\partial \phi} = -\frac{\partial V(\phi)}{\partial \phi}. \quad (8)$$

Hence, we obtain the Klein-Gordon equation

$$\partial_\mu \partial^\mu \phi + \frac{\partial V(\phi)}{\partial \phi} = 0. \quad (9)$$

In curved space-time, the Lagrangian density becomes

$$\mathcal{L} = a^3 \left(\frac{1}{2} \partial^\mu \phi \partial_\mu \phi - V(\phi) \right), \quad (10)$$

where a is the scale factor.

The Euler-Lagrange equation gives

$$\partial_\mu \frac{\partial \mathcal{L}}{\partial (\partial_\mu \phi)} - \frac{\partial \mathcal{L}}{\partial \phi} = 0, \quad (11)$$

$$\partial_\mu (a^3 \partial^\mu \phi) + a^3 \frac{\partial V}{\partial \phi} = 0, \quad (12)$$

$$3\dot{a}a^2\dot{\phi} + \ddot{\phi}a^3 - a^3 \nabla^2 \phi + a^3 \frac{\partial V}{\partial \phi} = 0. \quad (13)$$

We divide each term by a^3 , and substitute the Hubble parameter $H = \frac{\dot{a}}{a}$.

We then obtain the Klein- Gordon equation in curved space-time

$$\ddot{\phi} + 3H\dot{\phi} - \nabla^2 \phi + \frac{\partial V}{\partial \phi} = 0. \quad (14)$$

Appendix 3: The Langevin Equations

In this section, we derive the Langevin equations for the infrared fields. A similar demonstration is shown in [14].

Let's start from the definition of the infrared field given in (4.3)

$$\Phi(t, \vec{x}) = \int \frac{d^3k}{(2\pi)^3} \phi(t, \vec{k}) W(t, \vec{k}) e^{i\vec{k}\cdot\vec{x}}. \quad (15)$$

We differentiate Φ with respect to time

$$\dot{\Phi} = \int \frac{d^3k}{(2\pi)^3} \dot{\phi}(t, \vec{k}) W(t, \vec{k}) e^{i\vec{k}\cdot\vec{x}} + \int \frac{d^3k}{(2\pi)^3} \phi(t, \vec{k}) \dot{W}(t, \vec{k}) e^{i\vec{k}\cdot\vec{x}}, \quad (16)$$

and identify the first term as

$$\Pi = \int \frac{d^3k}{(2\pi)^3} \dot{\phi}(t, \vec{k}) W(t, \vec{k}) e^{i\vec{k}\cdot\vec{x}}, \quad (17)$$

and the second term as the noise term

$$s_\phi = \int \frac{d^3k}{(2\pi)^3} \phi(t, \vec{k}) \dot{W}(t, \vec{k}) e^{i\vec{k}\cdot\vec{x}}. \quad (18)$$

This gives the first Langevin equation

$$\dot{\Phi} = \Pi + s_\phi. \quad (19)$$

The equation for the conjugate field π is

$$\dot{\pi} + 3H\pi - \frac{\nabla^2 \phi}{a^2} + \frac{\partial V}{\partial \phi} = 0. \quad (20)$$

We can safely neglect the gradient term since we are in de-Sitter space with $a = e^{Ht}$ so the gradient term is exponentially suppressed.

Furthermore, we follow [14] and use the approximation

$$\frac{\partial V(\Phi)}{\partial \Phi} \sim \frac{\partial V(\phi)}{\partial \phi}, \quad (21)$$

otherwise, it would be necessary to simulate the evolution of the UV field as well. Our program, however, cannot simulate gradient terms as a full lattice simulation is required. We must therefore ignore the UV field.

We write equation (20) separating the IR Π and the UV $\delta\pi$ fields using (4.2)

$$\dot{\Pi} + \int \frac{d^3 k}{(2\pi)^3} \dot{\phi}(t, \vec{k}) \dot{W}(t, \vec{k}) e^{i\vec{k}\cdot\vec{x}} + \dot{\delta\pi} + 3H(\Pi + \delta\pi) + \frac{\partial V(\Phi)}{\partial \Phi} = 0. \quad (22)$$

We identify the conjugate noise term

$$s_\pi = \int \frac{d^3 k}{(2\pi)^3} \dot{\phi}(t, \vec{k}) \dot{W}(t, \vec{k}) e^{i\vec{k}\cdot\vec{x}}. \quad (23)$$

Finally, we separate the IR and the UV parts from (22) and obtain the second Langevin Equation

$$\dot{\Pi} + 3H\Pi + \frac{\partial V(\Phi)}{\partial\Phi} + s_\pi = 0, \quad (24)$$

with

$$\dot{\Pi} = \int \frac{d^3k}{(2\pi)^3} \dot{\pi}(t, \vec{k}) W(t, \vec{k}) e^{i\vec{k}\cdot\vec{x}}. \quad (25)$$

Appendix 4: Derivation of the noise correlation functions

In this section, we re-derive the noise correlation functions in the case of [15]. We use the window function presented in both articles [14, 15].

Expression of s_ϕ and s_π

We recall the definition of s_ϕ and s_π derived in the previous section

$$s_\phi = \int \frac{d^3k}{(2\pi)^3} \phi \dot{W} e^{i\vec{k}\cdot\vec{x}}, \quad (26)$$

and

$$s_\pi = \int \frac{d^3k}{(2\pi)^3} \dot{\phi} \dot{W} e^{i\vec{k}\cdot\vec{x}}, \quad (27)$$

where the dot means $\partial/\partial t$.

The window function W is the one used in [14, 15] and is given by

$$W = \theta(\epsilon a H - k), \quad (28)$$

where θ is the Heaviside step-function, and ϵ is a positive constant chosen to be less than 1.

We take the derivative of the step function with respect to time and obtain

$$\begin{aligned}\dot{W} &= \epsilon \dot{a} H \delta(\epsilon a H - k) \\ &= \epsilon a H^2 \delta(\epsilon a H - k),\end{aligned}\tag{29}$$

using the fact that $H = \dot{a}/a$ is constant and where $\delta(x)$ is the Dirac delta function.

We substitute equation (29) into (18) and (23) and obtain the expressions for s_ϕ and s_π :

$$s_\phi = \int \frac{d^3k}{(2\pi)^3} \phi e^{i\vec{k}\cdot\vec{x}} \epsilon a H^2 \delta(\epsilon a H - k),\tag{30}$$

and

$$s_\pi = \int \frac{d^3k}{(2\pi)^3} \dot{\phi} e^{i\vec{k}\cdot\vec{x}} \epsilon a H^2 \delta(\epsilon a H - k).\tag{31}$$

Expression of noise correlation functions

We substitute s_ϕ and s_π , derived above, into (4.7), where ϕ has been promoted to being an operator and is written explicitly in terms of creation and annihilation operators \hat{a}_k and \hat{a}_k^\dagger :

$$\begin{aligned}
S^\phi &= \int_t^{t+dt} dt \int_{t'}^{t'+dt'} dt' \iint \frac{d^3k d^3k'}{(2\pi)^6} \langle 0 | \left(\hat{a}_k \varphi_k + \hat{a}_k^\dagger \varphi_k^* \right) \left(\hat{a}_{k'} \varphi_{k'} + \hat{a}_{k'}^\dagger \varphi_{k'}^* \right) | 0 \rangle \\
&\times \dot{W}(t, k) \dot{W}(t', k') e^{i\vec{k} \cdot \vec{x}_1} e^{i\vec{k}' \cdot \vec{x}_2},
\end{aligned} \tag{32}$$

where φ_k is a function of k and t , and $\varphi_{k'}$ is a function of k' and t' .

All terms ending with $\hat{a}_k |0\rangle = 0$. Similarly, all terms beginning with $\langle 0 | \hat{a}_k^\dagger = 0$ (including the number operator $\hat{a}_k^\dagger \hat{a}_k$ since we are acting on the vacuum).

The only non-zero term is

$$\langle 0 | \hat{a}_k \varphi_k \hat{a}_{k'}^\dagger \varphi_{k'}^* | 0 \rangle = (2\pi)^3 \delta^3(k - k') |\varphi_k|^2. \tag{33}$$

Also, by defining $\vec{r} = \vec{x}_1 + \vec{x}_2$, we can compute the factor $e^{i\vec{k} \cdot (\vec{x}_1 + \vec{x}_2)}$.

Considering the spherical element:

$$\begin{aligned}
\int_0^\pi e^{ikr \cos \theta} \sin \theta d\theta &= \left[-\frac{e^{ikr \cos \theta}}{ikr} \right]_{\theta=0}^{\theta=\pi} \\
&= \frac{\sin kr}{kr},
\end{aligned} \tag{34}$$

then

$$\int_0^\pi e^{ikr \cos \theta} \sin \theta d\theta = j_0(kr), \tag{35}$$

where $j_0(kr) = \frac{\sin kr}{kr}$ is the zeroth order Bessel function.

We substitute equations (33) and (35) into (32) and obtain:

$$S^\phi = \int_t^{t+dt} dt \int_{t'}^{t'+dt'} dt' \iint \frac{d^3k d^3k'}{(2\pi)^3} j_0(kr) \delta^3(k - k') |\varphi_k|^2 \dot{W}(t, k) \dot{W}(t', k'). \tag{36}$$

We can now use the δ -function $\delta^3(k - k')$ to perform the integral over d^3k' . However, since we are only interested in the equal-time correlators, we can take $t = t'$. This allows us to motivate the expression of S^ϕ for a single time t from (36)

$$S^\phi = \int_t^{t+dt} dt \int \frac{d^3k}{(2\pi)^3} j_o(kr) |\varphi_k|^2 \dot{W}(t, k). \quad (37)$$

We substitute the expression for \dot{W} using equation (29):

$$S^\phi = \int_t^{t+dt} dt \int \frac{d^3k}{(2\pi)^3} j_o(kr) |\varphi_k|^2 \epsilon a H^2 \delta(\epsilon a H - k), \quad (38)$$

and we use equation 6 of [15], in order to compute $|\varphi_k|^2$

$$\varphi_k = \sqrt{\frac{\pi}{4k^3}} H e^{i(\frac{\pi}{2}\nu + \frac{\pi}{4})} \left(\frac{k}{aH}\right)^{3/2} H_\nu^1\left(\frac{k}{aH}\right), \quad (39)$$

where $H_\nu^1\left(\frac{k}{aH}\right)$ is the first order Hankel function.

This gives:

$$|\varphi_k|^2 = \frac{\pi}{4} \frac{1}{a^3 H} \left| H_\nu^1\left(\frac{k}{aH}\right) \right|^2, \quad (40)$$

which we substitute into 38 to obtain

$$S^\phi = \int_t^{t+dt} dt \int \frac{d^3k}{(2\pi)^3} j_o(kr) \frac{\pi}{4} \frac{\epsilon H}{a^2} \left| H_\nu^1\left(\frac{k}{aH}\right) \right|^2 \delta(\epsilon a H - k). \quad (41)$$

We write the volume element $d^3k = dk_1 dk_2 dk_3$, which in spherical coordinates gives : $d^3k = k^2 \sin\theta dk d\theta d\varphi$. The integrand, however, is independent of the angles θ and φ . We can therefore use the identity : $\int d^3k = 4\pi \int k^2 dk$.

Equation (41) becomes

$$S^\phi = \int_t^{t+dt} dt \int \frac{dk}{(2\pi)^2} k^2 j_o(kr) \frac{\pi \epsilon H}{2 a^2} \left| H_\nu^1 \left(\frac{k}{aH} \right) \right|^2 \delta(\epsilon aH - k). \quad (42)$$

We can now integrate equation (42) over k using the property of the δ -function and obtain

$$S^\phi = \int_t^{t+dt} \frac{dt}{(2\pi)^2} \epsilon^3 H^3 \frac{\pi}{2} j_o(\epsilon aHr) |H_\nu^1(\epsilon)|^2, \quad (43)$$

we use $dN = Hdt$ and the fact that H is constant to integrate with respect to time between t and $t + dt$ obtain Equation 10 from [15]

$$S^\phi = \left(\frac{H}{2\pi} \right)^2 dN \frac{\pi}{2} \epsilon^3 j_o(\epsilon aHr) |H_\nu^1(\epsilon)|^2. \quad (44)$$

Similarly for S^π , equation (38) is modified as

$$S^\pi = \int_t^{t+dt} dt \epsilon a H^2 \int \frac{d^3k}{(2\pi)^3} \delta(\epsilon aH - k) |\dot{\varphi}_k|^2 j_o(kr). \quad (45)$$

To compute $|\dot{\varphi}_k|^2$, we take the derivative with respect to time of (39):

$$\dot{\varphi}_k = -\sqrt{\frac{\pi}{4k^3}} H e^{i(\frac{\pi}{2}\nu + \frac{\pi}{4})} \frac{k}{a} \sqrt{\frac{k}{aH}} \left[\left(\frac{3}{2} - \nu \right) H_\nu^1 \left(\frac{k}{aH} \right) + \frac{k}{aH} H_{\nu-1}^1 \left(\frac{k}{aH} \right) \right], \quad (46)$$

where we have used [20], 9.1.27 : $\frac{d}{dz} [H_\nu^1(z)] = H_{\nu-1}^1(z) - \frac{\nu}{z} H_\nu(z)$.

Hence, we find

$$|\dot{\varphi}_k|^2 = \frac{\pi H}{4 a^3} \left| \left(\frac{3}{2} - \nu \right) H_\nu^1 \left(\frac{k}{aH} \right) + \frac{k}{aH} H_{\nu-1}^1 \left(\frac{k}{aH} \right) \right|^2. \quad (47)$$

As previously for S^ϕ , we use the identity $\int d^3k = 4\pi \int k^2 dk$, and obtain

$$S^\pi = \int_t^{t+dt} dt \epsilon a H^2 \int \frac{dk}{(2\pi)^2} 2k^2 |\dot{\varphi}_k|^2 j_o(kr) \delta(\epsilon a H - k). \quad (48)$$

We substitute for (47) and integrate over k using the δ -function and obtain

$$S^\pi = \int_t^{t+dt} \epsilon^3 \left(\frac{H^2}{2\pi} \right)^2 H dt \frac{\pi}{2} \left| \left(\frac{3}{2} - \nu \right) H_\nu^1(\epsilon) + \epsilon H_{\nu-1}^1(\epsilon) \right|^2 j_0(\epsilon a H r), \quad (49)$$

using $dN = H dt$, we integrate with respect to time between t and $t + dt$ and obtain the second results from Equation 10 in [15]:

$$S^\pi = \epsilon^3 \left(\frac{H^2}{2\pi} \right)^2 dN \frac{\pi}{2} \left| \left(\frac{3}{2} - \nu \right) H_\nu^1(\epsilon) + \epsilon H_{\nu-1}^1(\epsilon) \right|^2 j_0(\epsilon a H r). \quad (50)$$